

Efficient use of non-equilibrium measurement to estimate free energy differences for molecular systems

F. Marty Ytreberg and Daniel M. Zuckerman
*Center for Computational Biology and Bioinformatics,
 University of Pittsburgh, 200 Lothrop St., Pittsburgh, PA 15261*

(Dated: July 26, 2018)

A promising method for calculating free energy differences ΔF is to generate non-equilibrium data via “fast-growth” simulations or experiments – and then use Jarzynski’s equality. However, a difficulty with using Jarzynski’s equality is that ΔF estimates converge very slowly and unreliably due to the nonlinear nature of the calculation – thus requiring large, costly data sets. Here, we present new analyses of non-equilibrium data from various simulated molecular systems exploiting statistical properties of Jarzynski’s equality. Using a fully automated procedure, with no user-input parameters, our results suggest that good estimates of ΔF can be obtained using 6-15 fold less data than was previously possible. Systematizing and extending previous work [1], the new results exploit the systematic behavior of bias due to finite sample size. A key innovation is better use of the more statistically reliable information available from the raw data.

I. INTRODUCTION

The calculation of free energy differences, ΔF plays an essential role in many fields of physics, chemistry and biology [1, 2, 3, 4, 5, 6, 7, 8, 9, 10, 11, 12, 13, 14, 15, 16, 17]. Examples include determination of the solubility of small molecules, and binding affinities of ligands to proteins. Rapid and reliable estimates of ΔF would be particularly valuable to structure-based drug design, where current approaches to virtual screening of candidate compounds rely primarily on ad-hoc methods [18, 19]. Free energy estimates are also critical for protein engineering [20, 21].

The focus of this report is non-equilibrium “fast-growth” free energy calculations [1]. These methods hold promise – yet to be fully realized – for very rapid estimation of ΔF . The central idea behind the non-equilibrium methods is to calculate the *irreversible* work during a very rapid (thus non-equilibrium) switch between the two systems or states of interest. Multiple switches are done, and the resulting set of work values can be used to estimate ΔF using Jarzynski’s equality (detailed in Sec. II) [22].

Somewhat surprisingly, non-equilibrium ΔF calculations are critical for analyzing single-molecule pulling *experiments* [7, 15]. In essence, these experiments generate non-equilibrium work values, as pointed out by Hummer and Szabo, so the only way to estimate the free energy profile is to use Jarzynski’s equality [7, 23]. The methods that we develop in this report should be equally useful for analyzing such experiments.

It has been accepted for some time that there are three sources of error [24] for non-equilibrium ΔF calculation: (i) inaccuracy of the force field [25], (ii) inadequate sampling of the configurational space [26, 27, 28, 29, 30], and (iii) bias due to finite sample size [1, 31, 32, 33, 34, 35]. Error in free energy calculations have been of long-standing interest, e.g. Refs. [36, 37, 38, 39, 40]

The present study addresses only source (iii), and attempts to determine the most efficient use of fast-growth work values. In other words, given a (finite) set of work values generated by simulation or experiment, what is the best estimate for ΔF ? We do not here attempt to prescribe the best method for generating non-equilibrium work values.

We proceed by first introducing two new block averaging techniques, based on the original proposal by Wood *et al.* [41]. Block averaging provides well-behaved, but biased, ΔF estimates. We then discuss two distinct schemes for extrapolating to the “infinite data limit”. Our work systematizes and extends previous work by Zuckerman and Woolf [1], who originally proposed the use of block averages for extrapolation.

Methods to lessen the effect of bias due to finite sample size have been proposed for the case when switching between systems is performed in both directions [42, 43, 44], and for the simplified case in which the non-equilibrium work values follow a quasi-Gaussian distribution [16, 45]. Hummer also considered errors in non-equilibrium ΔF calculations [46]. To our knowledge, however, other workers have not addresses uni-directional switching in highly non-Gaussian systems.

The techniques outlined in the following sections offer rapid estimates for ΔF for the systems we studied – namely, the chemical potential for a Lennard-Jones fluid, “growing” a chloride ion in water, methanol \rightarrow ethane in water, and palmitic \rightarrow stearic acid in water. Work values for these systems follow highly non-Gaussian distributions. We compare our extrapolated results to ΔF obtained by using Jarzynski’s equality, finding a 6-15 fold decrease in the the number of work values needed to estimate ΔF for the test systems considered here.

II. FAST-GROWTH

Fast-growth techniques have been described in detail elsewhere [1, 22, 46], so we will simply outline the method. Consider two systems defined by potential energy functions U_0 and U_1 . To calculate the free energy difference ΔF between these two systems, one must simply “switch” the system from U_0 to U_1 . This is readily accomplished by defining a switching parameter λ such that

$$U_\lambda(\mathbf{x}) = U_0(\mathbf{x}) + \lambda[U_1(\mathbf{x}) - U_0(\mathbf{x})], \quad (1)$$

where \mathbf{x} is a set of configurational coordinates, and $U_\lambda(\mathbf{x})$ describes the “hybrid” potential energy function for all values of λ from 0 to 1. We note that nonlinear scaling with λ is also possible [5, 6, 13, 14, 47] resulting in hybrid potentials differing from Eq. (1). Our approach here also applies, in principle, to other such choices. Essentially, the idea behind fast-growth methods is to perform rapid switches from $\lambda = 0 \rightarrow 1$, where each switch is generated starting from coordinates drawn from the equilibrium ensemble for $\lambda = 0$. During each switch, the irreversible work is accumulated, generating a single work value. Multiple switches are done to generate a distribution of these work values $\rho(W)$.

A. Simple Estimators

It has been appreciated for some time that the average work obtained over many such switches provides a rigorous upper bound for the free energy difference,

$$\Delta F \leq \langle W \rangle_0, \quad (2)$$

where the $\langle \dots \rangle_0$ represents an average over many switches starting from the equilibrium ensemble for $\lambda = 0$ and ending at $\lambda = 1$. Equality occurs only in the limit of infinitely slow switches. Further, if the distribution of work values $\rho(W)$ is Gaussian (this occurs if the system remains in equilibrium during the switch, but also may occur in certain far from equilibrium situations), then the high temperature expansion of Zwanzig [48] gives

$$\Delta F = \langle W \rangle_0 - \frac{1}{2}\beta\sigma_W^2, \quad (3)$$

where σ_W is the standard deviation of $\rho(W)$, and $\beta = 1/k_B T$ where T is the temperature of the system and k_B is the Boltzmann constant.

However, for the fast-growth work values under consideration here, the distribution of work values can be very broad and non-Gaussian. Thus Eqs. (2) and (3) will not provide reasonable estimates of ΔF ; see Fig. 1. It is possible to use higher order moments to estimate ΔF (see for example Refs. [16, 45, 48, 49]). These estimators are most useful in the near-equilibrium regime.

B. Jarzynski Equality

Due to recent work by Jarzynski [22, 50, 51], it is possible to estimate ΔF using these fast-growth W values via

$$e^{-\beta\Delta F} = \left\langle e^{-\beta W} \right\rangle_0, \quad (4)$$

This remarkable relationship is valid for *arbitrary* switching speed, implying that one can perform switches as rapidly as desired and still obtain valid estimates of ΔF . The Jarzynski equality thus provides an estimate for ΔF for a set of N work values given by

$$\Delta F_{Jarz} = -\frac{1}{\beta} \ln \left[\frac{1}{N} \sum_{i=1}^N e^{-\beta W_i} \right], \quad (5)$$

The ΔF estimates given by Eq. (5), however, are very sensitive to the distribution of work values $\rho(W)$ [1, 31, 32]. If the width of the work distribution large, i.e. $\sigma_W \gg k_B T$ (this implies a very rapid switch and/or a complex system), then often thousands, or even tens of thousands of work values are needed to reliably estimate ΔF . An example of this can be seen in Fig. 1 where a histogram of work values is shown for PAL2STE (described in Sec. IV). The value

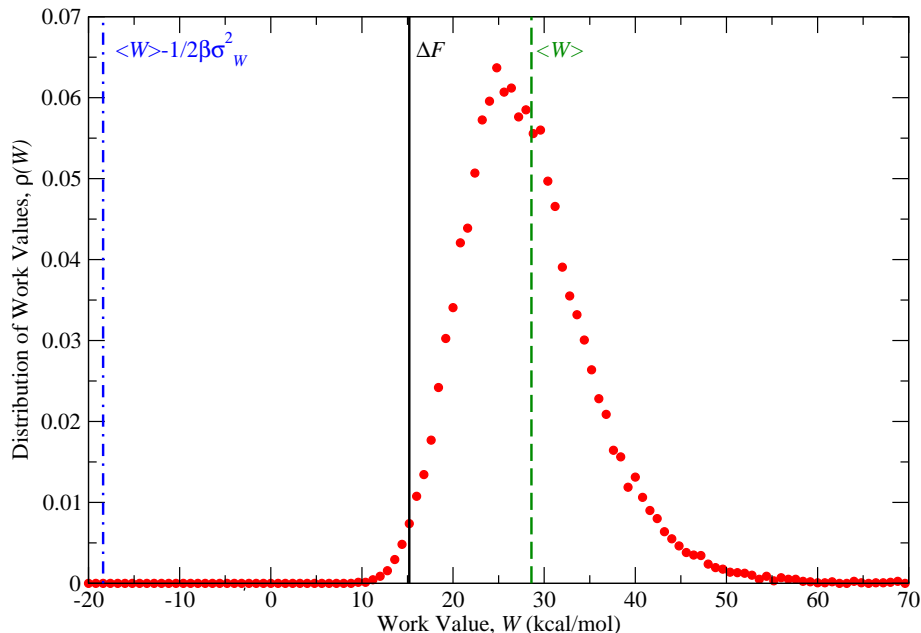


FIG. 1: Distribution of work values for PAL2STE test system (palmitic \rightarrow stearic acid mutation in water, described in Sec. IV). Also included in this plot are the estimators given by Eqs. (2) and (3) shown by the blue dot-dash and green dashed line respectively. The solid black line shows the ΔF estimate obtained by using Jarzynski’s equality in Eq. (5) for all available data.

of ΔF_{Jarz} given by the Jarzynski equality, as well as estimators $\langle W \rangle_0$ and $\langle W \rangle_0 - \frac{1}{2}\beta\sigma_W^2$, are shown on this plot. This graphically demonstrates why Eqs. (2) and (3) are often poor estimates of the free energy for fast-growth work values.

If the switch is performed instantaneously, then Eq. (5) becomes

$$e^{-\beta\Delta F} = \left\langle e^{-\beta[U_1(\mathbf{x}) - U_0(\mathbf{x})]} \right\rangle_0, \quad (6)$$

often called single-stage free energy perturbation [48, 52]. In this limit, the system is not allowed to relax at any intermediate values of λ . Instead $U_1(\mathbf{x})$ is simply evaluated at values of \mathbf{x} drawn from the equilibrium ensemble for $\lambda = 0$. The advantage of this method is that data can be generated very quickly. However, in practice, unless there is sufficient overlap between the states described by U_0 and U_1 , the estimate of ΔF will be biased, often by many $k_B T$ [53, 54]. The problem of attaining overlap of states can be improved by drawing from the equilibrium ensemble for an unphysical “soft-core” state (such as for $\lambda = 0.5$) [28, 47].

Recent work by Hendrix and Jarzynski [50] showed that essentially the only determining factor in the accurate calculation of ΔF was physical CPU time spent during the calculation. So, doing many rapid switches has no advantage over doing fewer slower switches. This conclusion is based upon using Eq. (5) for all ΔF estimates.

This manuscript describes methods that exploit statistical properties of Jarzynski’s equality, allowing us to do use work values from very rapid switches and obtain ΔF estimates with 6-15 fold less work values than using Eq. (5).

III. OTHER METHODS

To calculate reliable ΔF estimates using less work values, one can generate a narrower $\rho(W)$, i.e. perform the switching process more slowly. However, slower switching speed means that more computational time will be spent to generate each work value – offsetting some of the advantage gained by doing rapid switches.

If the switch is performed so slowly that the system remains near equilibrium during the switch, then the width of the distribution will be very small ($\sigma_W < k_B T$), and thus only a few work values are required for accurate estimation of ΔF [34, 55]. This slow-growth method is, in principle, equivalent to thermodynamic integration [56] where ΔF is

calculated by allowing the system to reach equilibrium for each value of λ . Then ΔF is found using

$$\Delta F = \int_0^1 d\lambda \left\langle \frac{\partial U_\lambda(\mathbf{x})}{\partial \lambda} \right\rangle_\lambda. \quad (7)$$

Thermodynamic integration and slow-growth can provide very accurate ΔF calculations, but are also computationally expensive [6, 14, 29, 57].

As previously mentioned, the equilibrium ensemble, when using the Eq. (5), is generated for $\lambda = 0$. Then $\rho(W)$ is generated by doing switches from $\lambda = 0 \rightarrow 1$ (forward switches) with configurations drawn from the $\lambda = 0$ ensemble. It is also possible to generate another equilibrium ensemble for $\lambda = 1$ and then perform *reverse* switches from $\lambda = 1 \rightarrow 0$. It has been shown that, if one combines the use of the forward and reverse work values, convergence is much more rapid than doing just forward switches [42, 43, 44, 58]. It has been recently demonstrated that most efficient use of forward and reverse work values is for Bennett’s method [3, 42, 43].

There is, however, a distinct advantage to using Jarzynski’s estimates with only forward switches, when one considers the eventual goal of predicting relative binding affinities for application in drug design. In this situation, if using Jarzynski estimates, one need only generate a single high-quality equilibrium ensemble for a particular ligand-receptor or reference complex. Then one can determine relative binding affinities for other ligands without generating another equilibrium ensemble – a significant decrease in computational expense.

IV. TEST SYSTEMS

To show the generality of the methods proposed in this study we consider four test systems with varying molecular complexity: a chemical potential calculation for a Lennard-Jones fluid, “growing” a chloride ion in water, methanol \rightarrow ethane in water, and stearic \rightarrow palmitic acid in water.

The last two systems are alchemical mutations of fully solvated molecules (see Refs. [1, 59] for simulation details), and the first system is a chemical potential calculation done by the particle insertion method (see Ref. [50] for details). All three of these data sets were generated previous to this study [60].

The growing chloride system was studied using TINKER version 4.1 [61], with the simulation conditions chosen to closely match those of Lybrand *et al.* in Ref. [57]. Stochastic dynamics simulations were carried out in the canonical ensemble (constant N, V, T) in a cubic box of edge length 18.6216 Å. The temperature was held at 300 K by a Berendsen thermostat with a time constant of 0.1 [62]. The chloride ion was modeled with Lennard-Jones parameters $\sigma = 4.4463$ Å and $\epsilon = 0.1070$ kcal/mol, and was solvated by 214 SPC water molecules. Ewald summation approximated charge interactions and RATTLE was used to hold the water molecules rigid [63]. For this test system, the Lennard-Jones “size” was increased by 1.0 Å, from $\sigma = 4.4463$ Å at $\lambda = 0$ to $\sigma = 5.4463$ Å at $\lambda = 1$.

To obtain fast-growth work values, a time step of 1.0 fs was used. The system was equilibrated for at least 10 ps, after which starting configurations for each fast-growth trajectory were generated every 100 time steps.

Below we list the notation used to refer to each data set. Also included are statistical features of the data sets – the total number of work values (N_{tot}), the mean work ($\langle W \rangle$) and the standard deviation (σ_W). These data sets are all considered difficult to use for ΔF calculations owing to the facts that $\sigma_W \gg k_B T$ and $\langle W \rangle - \Delta F > 10k_B T$; see Eqs. (2) and (3) and Fig. 1.

LJ – Chemical potential calculation for a Lennard-Jones fluid in 1 λ -step [50]. This corresponds to instantaneous switching or free energy perturbation, as described in sec. II. $N_{tot} = 100,000$, $\langle W \rangle = 305.1 k_B T$ and $\sigma_W = 83.5 k_B T$. Using all work values, Eq. (5) gives a best estimate $\Delta F_{best} = 0.7 k_B T$.

GROWCL – Grow chloride by 1.0 Å in 10 λ -steps with 1 relaxation step at each value of λ . $N_{tot} = 40,000$, $\langle W \rangle = 40.1$ kcal/mol and $\sigma_W = 8.6$ kcal/mol. Using all work values, Eq. (5) gives $\Delta F_{best} = 18.4$ kcal/mol.

METH2ETH – Methanol to ethane mutation data using 200 λ -steps with 1 dynamic relaxation step at each value of λ [1]. $N_{tot} = 9,600$, $\langle W \rangle = 37.0$ kcal/mol and $\sigma_W = 12.3$ kcal/mol. Using all work values, Eq. (5) gives $\Delta F_{best} = 7.4$ kcal/mol.

PAL2STE – Palmitic to Stearic acid mutation data using 55 λ -steps with 10 relaxation steps at each value of λ [59]. $N_{tot} = 20,000$, $\langle W \rangle = 28.6$ kcal/mol and $\sigma_W = 7.5$ kcal/mol. Using all work values, Eq. (5) gives $\Delta F_{best} = 15.2$ kcal/mol.

Since the goal is to determine the best analysis for a given set of work values, we assume that the true ΔF is given by Eq. (5) using all available work values (i.e. ΔF_{best} above). Determining whether the distribution of work values $\rho(W)$ used in this paper are complete and representative is beyond the scope of this report.

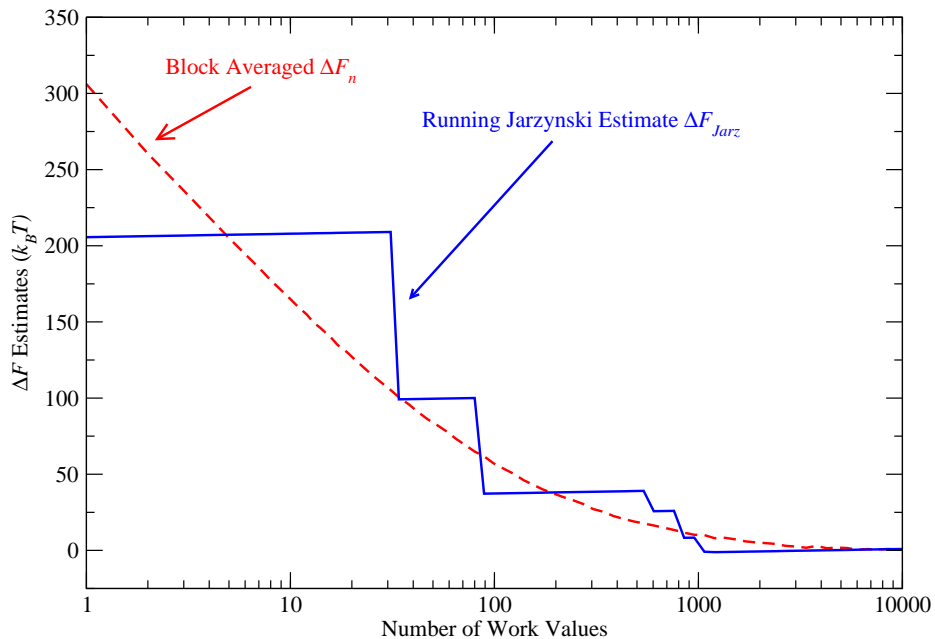


FIG. 2: The running Jarzynski estimate, given by Eq. (5), as a function of the number of work values used in the estimate, N is shown as a solid blue line. The dashed red line shows the sub-sampled block averaged free energy estimate given by Eq. (9), plotted as a function of the number of work values in each block, n . Data used for these estimate were obtained from the LJ test system (chemical potential for a Lennard-Jones fluid). The Jarzynski estimate displays erratic convergence behavior, while the block averaged free energy estimate displays a smooth monotonically decreasing estimate

V. BLOCK AVERAGING

The motivation for using block averages can be seen in Fig. 2 (see also Refs. [2, 41]). The solid blue line is a running estimate for ΔF obtained by using Eq. (5) and the dashed red line is obtained by block averaging. Both curves are obtained using the LJ test system. The running Jarzynski estimate exhibits very poor convergence behavior, making it very difficult to establish when a reliable estimate of ΔF has been obtained. The block averaged free energy, however, displays a smooth monotonically decreasing ΔF estimate, which approaches the true ΔF .

Each block averaged free energy (ΔF_n) data point was obtained from a set of N work values (W_1, W_2, \dots, W_N) using the following scheme [41]:

1. Draw n work values at random from the set, generating a subset (W_1, W_2, \dots, W_n). This is now the j^{th} block of work values.
2. Use Jarzynski's equality, Eq. (5) to obtain a free energy estimate F_j for this block

$$F_j = -\frac{1}{\beta} \ln \left(\sum_{i \in \text{block } j} e^{-\beta W_i} \right). \quad (8)$$

3. Repeat steps 1 and 2 until you have m blocks, each containing n values. Now the average (ΔF_n) and standard deviation (σ_n) can be calculated using

$$\Delta F_n = \frac{1}{m} \sum_{j=1}^m F_j = \frac{1}{m} \sum_{j=1}^m \left[-\frac{1}{\beta} \ln \left(\sum_{i \in j} e^{-\beta W_i} \right) \right], \quad (9)$$

$$\sigma_n^2 = \frac{n}{N} \sum_{j=1}^m (F_j - \Delta F_n)^2. \quad (10)$$

This process is carried out for every possible value of n (i.e. $n = 1, 2, 3, \dots, N$).

In previous work [1, 41], $m = N/n$ was chosen, i.e. m is the number of blocks of size n from a data set of size N . The weakness of this choice is that a reshuffling of the data set gives a new (generally different) set of ΔF_n values. To avoid this weakness we choose m large enough that the resulting ΔF_n values do not depend upon the value of m . This is typically accomplished with $m \sim 100 \times N/m$.

Since there are two distinct ways of randomly drawing from a data set (i.e. implementing the first step above), we introduce two new block averaging schemes. The first is to draw work values from (W_1, W_2, \dots, W_N) at random *with replacement* – i.e. it is possible to draw a particular work value more than once. We call this a bootstrapped ΔF_n [64]. The second is to draw from (W_1, W_2, \dots, W_N) at random *without replacement*. We call this a sub-sampled ΔF_n [65].

The difference between the bootstrapped and sub-sampled methods can be illustrated by considering a data set of N work values where $N - 1$ values are large and one value is very small. Due to the highly nonlinear nature of the Jarzynski equality, the single small work value will dominate Eq. (9). Suppose one calculates ΔF_n for $n = N$ using both of these methods. The sub-sampled method will only have one ΔF_N estimate since reshuffling the work values has no effect when $n = N$. However, the bootstrapped method calculates a ΔF_N value that is larger than the sub-sampled ΔF_N due to the fact that it will draw the small work value only a fraction of the time. A generalization of this argument shows that the bootstrapped ΔF_n will exceed the sub-sampled ΔF_n for every value of n .

VI. EXTRAPOLATION METHODS

Now that a smooth function has been obtained in the block averaged free energy ΔF_n , shown in Fig. 2, extrapolation to the infinite data limit becomes feasible, as originally suggested by Zuckerman and Woolf [1]. The basic idea is to plot ΔF_n as a function of some variable and then extrapolate to the infinite data limit ($n \rightarrow \infty$). It is useful to plot ΔF_n as a function of $\chi = 1/n^\tau$ as shown in Fig. 3 [1]. The plot was generated by choosing 100 work values at random from the PAL2STE data set. ΔF_n was then computed for this subset of 100 work values following the steps outlined in Sec. V. In this plot the *bootstrapped* ΔF_n is shown, and the best estimate ΔF_{best} is included as the solid black line. A value of $\tau = 0.22$ was chosen to minimize the slope of $\Delta F_n(\chi)$ as discussed below. The errorbars show the statistical uncertainty of the ΔF_n given by the standard error associated with σ_n in Eq. (10). The smallest uncertainty occurs for $\chi = n = 1$ due to the fact that $\Delta F_n(\chi = 1)$ is simply the average work.

It is useful to plot ΔF_n as a function of $\chi = 1/n^\tau$ as in Fig. 3 (rather than n) because the infinite data limit ($n \rightarrow \infty$) now corresponds to $\chi = 0$. In addition, this simple form gives a bounded interval ($\chi = (0, 1]$), rather than an infinite one (such as ΔF_n as a function of n). This form allows us to develop two simple extrapolation schemes as explained in the following sections.

A. Linear Extrapolation

It is known that the block averaged free energy ΔF_n in Eq. (9) guarantees monotonic behavior [1, 2, 24]. Thus, one can hope to obtain a reasonable estimate of ΔF by simply continuing the curve in Fig. 3 with a straight line. Such a linear extrapolation guarantees that our extrapolated results will not exceed ΔF_n for $n = N$ – necessary since ΔF_n is a rigorous upper bound for the true ΔF [24].

We test this extrapolation method using the test systems described in IV. This *fully automated* process contains the following steps: (i) Draw a subset containing N work values (W_1, W_2, \dots, W_N) at random from the data set. (ii) Plot the *bootstrapped* ΔF_n as a function of $\chi = 1/n^\tau$; vary τ , then choose the value of τ that minimizes the slope of the tail (i.e. small χ) of ΔF_n . (If one has enough data to get the correct ΔF then, for the right value of τ , the slope will be nearly zero.) (iii) Extrapolate ΔF_n to $\chi = 0$ using a straight line. The intercept ($\chi = 0$) is our extrapolated free energy ΔF_{lin} . (iv) Using these same N work values, estimate the free energy ΔF_{Jarz} with Eq. (5). This process is repeated 500 times to obtain the average and standard deviation of our ΔF_{lin} and ΔF_{Jarz} .

A simple extension of the linear method shown here, is to fit ΔF_n to a nonlinear function, such as quadratic in χ , as in previous work by Zuckerman and Woolf [1]. These nonlinear extrapolation methods offer little, if any, improvement in the average ΔF extrapolations. And, due to the inherent instability of high order fits, the standard deviations for the extrapolated results are much larger than those obtained for linear extrapolation.

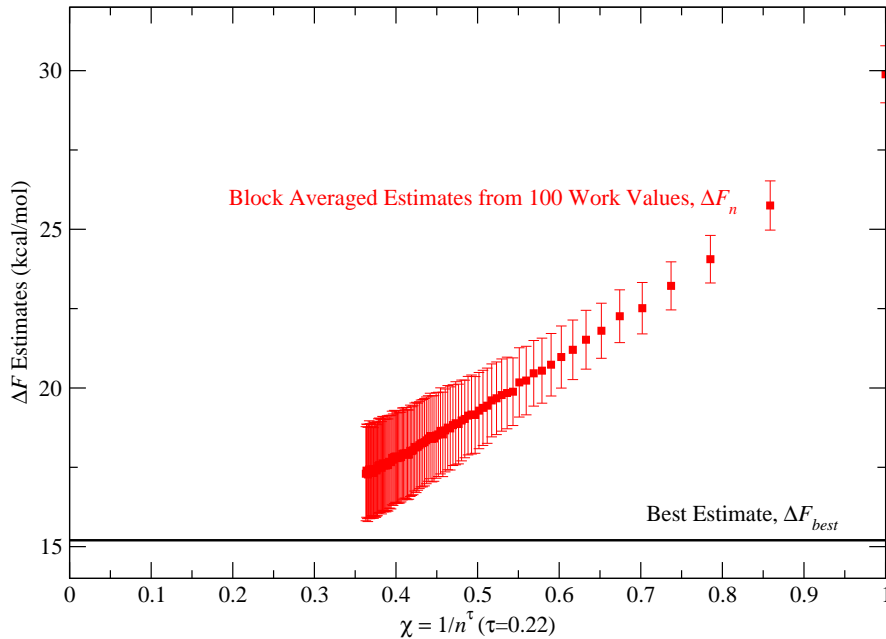


FIG. 3: Bootstrapped block averaged free energy (ΔF_n), given by Eq. (9) as a function of χ are shown as red squares. The solid black line represents the best estimate ΔF_{best} . The value of $\tau = 0.22$ is chosen to minimize the slope of $\Delta F_n(\chi)$ as described in Sec. VIA. This plot was generated using 100 work values chosen at random from the PAL2STE test system (palmitic \rightarrow stearic acid mutation). In this plot, extrapolating to the infinite data limit corresponds to continuing the ΔF_n curve to $\chi = 0$ to obtain the intercept. This plot also demonstrates that the large χ (small n) data are more reliable as shown by the errorbars which represent the standard error of ΔF_n .

B. Reverse Cumulative Integral Extrapolation

As previously mentioned (see Fig. 3), the most precise ΔF_n values occur for larger $\chi \approx 1$ (i.e. smaller n), yet the previous linear extrapolation scheme relies exclusively on small χ values. Thus, in an effort to use the more precise large- χ data to extrapolate ΔF , we now formulate an integration scheme which explicitly includes all values of χ .

Consider treating ΔF_n in Fig. 3 as a smooth function $\Delta F_n(\chi)$, from $\chi = 0$ to 1. We are free to consider the area under this function, re-written using integration by parts,

$$\int_0^1 d\chi \Delta F_n(\chi) = \int_0^1 d\chi (1 - \chi) \frac{d\Delta F_n(\chi)}{d\chi} + \Delta F_n(\chi = 0). \quad (11)$$

But $\Delta F_n(\chi = 0)$ is just the extrapolated free energy estimate ΔF_{rci} , so

$$\Delta F_{rci} = \int_0^1 d\chi \left(\Delta F_n(\chi) - (1 - \chi) \frac{d\Delta F_n(\chi)}{d\chi} \right). \quad (12)$$

Now the *reverse cumulative integral* function can be defined by

$$RCI(\chi) = \int_1^\chi d\chi' \left(\Delta F_n(\chi') - (1 - \chi') \frac{d\Delta F_n(\chi')}{d\chi'} \right), \quad (13)$$

where it should be noted that we accumulate in the reverse direction from $\chi' = 1$, where the data is most precise, to $\chi' = \chi$, i.e. from right to left in Figs. 3 and 4.

A sample plot of the reverse cumulative integral is shown in Fig. 4. This plot was generated using two *subsets* (represented by open and closed symbols) of 100 work values drawn at random from the PAL2STE data set. The solid black line shows the best estimate ΔF_{best} , the blue squares are the sub-sampled ΔF_n and the red circles are $RCI(\chi)$. For each of the two subsets, the value of τ was chosen to minimize the slope of the tail of $RCI(\chi)$, as discussed below. The subset represented by the open symbols slightly overestimates ΔF_{best} , while the subset represented by the closed symbols slightly underestimates ΔF_{best} .

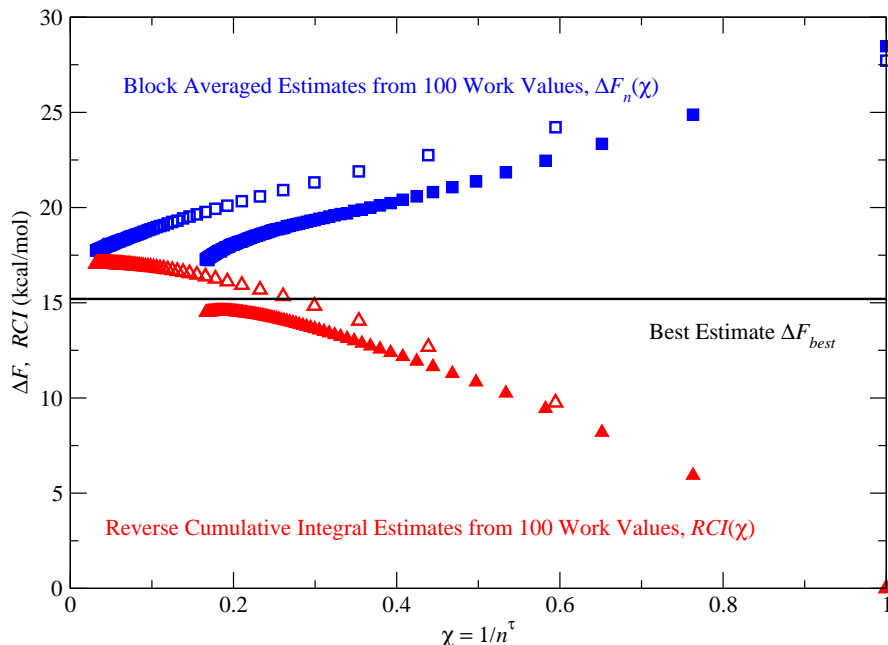


FIG. 4: Examples of the reverse cumulative integral, $RCI(\chi)$ are shown for a two *subsets* of 100 work values drawn at random from the PAL2STE data set (palmitic to stearic acid mutation). The first subset is represented by open symbols and the second by closed symbols. The solid black line shows the best estimate ΔF_{best} , the blue squares are the sub-sampled ΔF_n and the red circles are the $RCI(\chi)$. The strength of using $RCI(\chi)$ for extrapolation is its explicit use of all the ΔF_n values. For each subset, the value of τ was chosen to minimize the slope of the small- χ tail of $RCI(\chi)$, as described in Sec. VI B. In this example, the subset represented by the open symbols slightly overestimates ΔF_{best} , while the subset represented by the closed symbols slightly underestimates ΔF_{best} .

To obtain an extrapolated value for ΔF , consider the case where one has more than enough data to obtain ΔF exactly. In this situation, *if τ is chosen carefully*, $RCI(\chi)$ will have nearly zero slope for small χ , since accumulating more χ values will not change the estimate. Thus, one can hope to extrapolate ΔF by simply finding a value of τ where the slope $dRCI(\chi)/d\chi$ is the smallest for small χ , then the extrapolated free energy ΔF_{rci} will be the value of $RCI(\chi)$ for the smallest value of χ available, χ_{min} .

Our fully automated test of this new extrapolation method is very similar to that described in the previous section, with only minor differences: (i) the *sub-sampled* ΔF_n is used, (ii) the value of τ is chosen to minimize the slope of the tail (small χ) of $RCI(\chi)$ – see Fig. 4, and (iii) once the value of τ is determined, the free energy is estimated to by $\Delta F_{rci} = RCI(\chi_{min})$. Comparison is made with the Jarzynski estimate ΔF_{Jarz} using the same procedure as in the last section.

VII. RESULTS

The initial results of this study are very positive as shown by the rapid convergence of our extrapolated ΔF estimates (Fig. 5). Compared to ΔF_{Jarz} , estimates of ΔF can be made with 6-15 fold less work values, i.e. less computational expense.

Fig. 5 demonstrates how the linear and reverse cumulative extrapolation (RCI) methods described above compare to using the Jarzynski estimate of Eq. (5), for each of the four test systems. For all of the plots shown, the solid black horizontal line corresponds to the Jarzynski estimate using all available work values and thus represents the best estimate ΔF_{best} from Sec. IV. The red squares are averages of ΔF_{Jarz} using Eq. (5), the blue triangles are averages of ΔF_{lin} from Sec. VI A, and the green circles are averages of ΔF_{rci} from Sec. VI B. The inset for each plot shows the standard deviation of the ΔF estimates ($\sigma_{\Delta F}$). Averages and standard deviations were obtained by performing 500 independent trials for each estimate (ΔF_{Jarz} , ΔF_{lin} , ΔF_{rci}) for every value of N . Thus $\sigma_{\Delta F}$ indicates the expected statistical uncertainty – that is the range of values one would expect if the calculation was performed *de novo*.

A glance at Fig. 5 reveals that the linearly extrapolated ΔF_{lin} estimates converge to the best estimate ΔF_{best} more quickly than the Jarzynski estimate ΔF_{Jarz} . The larger uncertainty of the linearly extrapolated estimates is, at least partially, explained by the fact that it relies on the less certain ΔF_n values as explained in Sec. VI A. Also, the linear

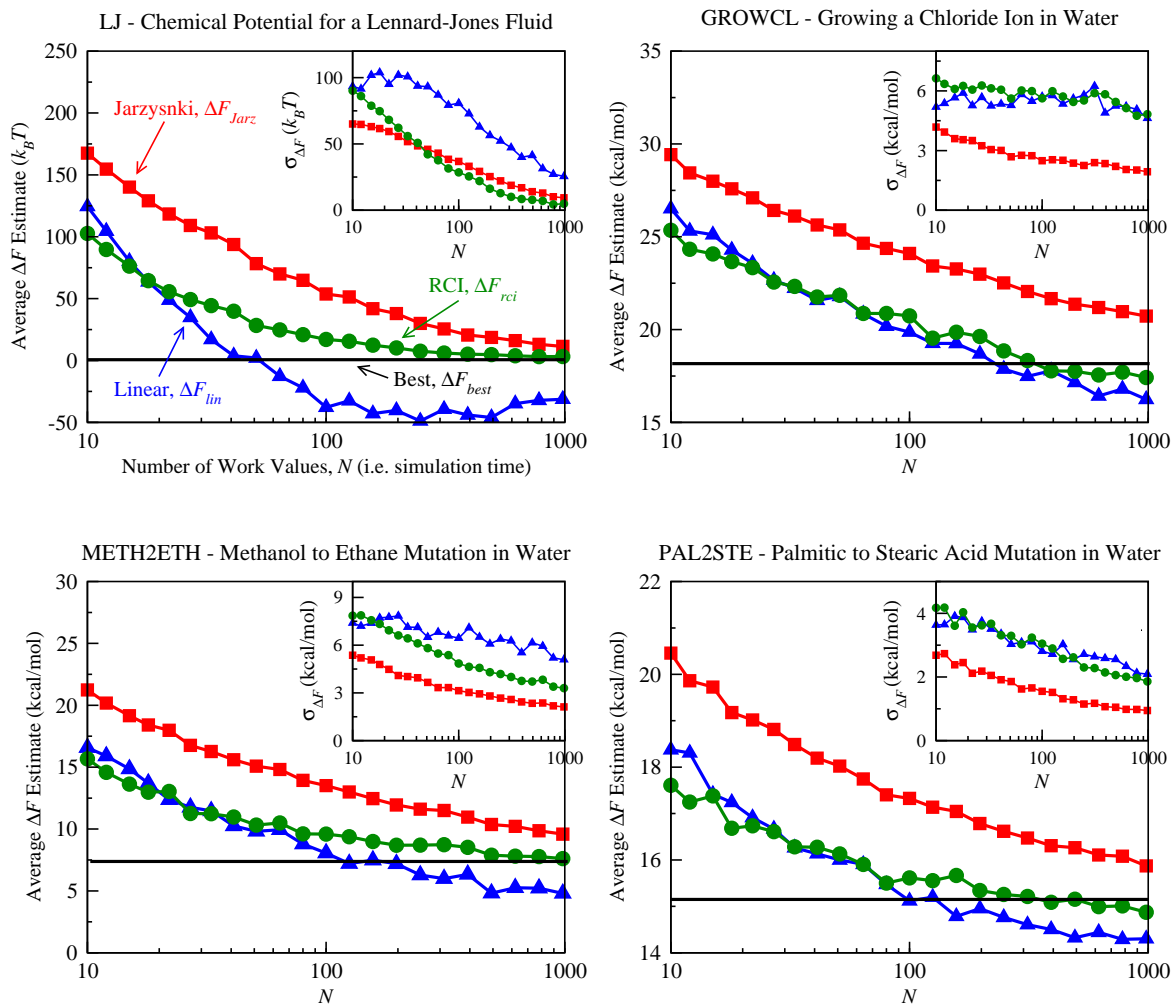


FIG. 5: A comparison between ΔF estimates for linear extrapolation, reverse cumulative integral (RCI) extrapolation, and the Jarzynski equality for all of the test systems. For each of the plots the solid horizontal black line indicates the best estimate ΔF_{best} given in Sec. IV, the red squares are averages of Jarzynski estimates given by Eq. (5), the blue triangles are averages of linearly extrapolated estimates from Sec. VIA, and the green circles are averages of RCI extrapolated estimates from Sec. VIB. The inset in each plot shows the standard deviation for each of the estimates. Averages and standard deviations were obtained by performing 500 independent trials for each estimate for each value of N .

estimates tend to “overshoot” ΔF_{best} .

Many of the disadvantages of the linearly extrapolated estimates are somewhat overcome by RCI extrapolation. Since RCI extrapolation relies heavily on the more precise values of ΔF_n , the uncertainty is generally smaller than that of the linear estimates. Remarkably, for the LJ system, the RCI extrapolated uncertainty is smaller than the Jarzynski estimate uncertainty for $N > 40$. Also, RCI extrapolated estimates do not tend to appreciably overshoot ΔF_{best} .

To obtain a quantitative comparison between RCI extrapolated estimates ΔF_{rci} , and Jarzynski estimates ΔF_{Jarz} , we ask the following question: how many work values are necessary to obtain a ΔF estimate that falls within 1.0 kcal/mol of the best estimate ΔF_{best} ? Table I summarizes the results of this comparison. The RCI estimates offer a significant improvement over the Jarzynski estimates in all of the test systems, with a 6-15 fold decrease in the number of work values needed to estimate ΔF_{best} within 1.0 kcal/mol.

Due to the fact that the linearly extrapolated estimates tend to overshoot ΔF_{best} , often by many kcal/mol, a quantitative comparison between ΔF_{lin} and ΔF_{Jarz} would be difficult and unreliable. Thus, we do not attempt to make such a comparison here.

TABLE I: A quantitative comparison between the reverse cumulative integral estimates (ΔF_{rci}) and the Jarzynski estimate (ΔF_{Jarz}) shown in Fig. 5. The first column shows the test system used in the comparison. The second and third columns are the number of work values needed to obtain an estimate that falls within 1.0 kcal/mol of ΔF_{best} for the reverse cumulative integral (N_{rci}) and Jarzynski (N_{Jarz}) estimates. The rightmost column is the ratio of these two values, i.e. the approximate improvement of the reverse cumulative integral estimate over the Jarzynski estimate.

System	N_{rci}	N_{Jarz}	Improvement
LJ	800	6000	7.5
GROWCL	200	3000	15
METH2ETH	400	2500	6.25
PAL2STE	40	500	12.5

VIII. CONCLUSION

We have described two methods that improve standard non-equilibrium estimates of free energy differences, ΔF : linear extrapolation and reverse cumulative integral (RCI) extrapolation. Four test systems were used in this study: chemical potential calculation for a Lennard-Jones fluid, growing a chloride ion in water, methanol \rightarrow ethane mutation in water, and palmitic \rightarrow stearic acid mutation in water. Both of the methods rely on block averaged free energies ΔF_n , which are extrapolated to the infinite data limit, and offer more rapid estimates of ΔF than using the Jarzynski equality alone, for the test systems considered here.

Previous work by Zuckerman and Woolf [1] used a quadratic extrapolation method to estimate ΔF . The present study offers several improvements: (i) the accuracy and uncertainty of the extrapolated estimates are reduced due to improved, fully automated methods; (ii) two new methods for calculating the block averaged free energies, ΔF_n are described; (iii) a key innovation is offered in RCI extrapolation in its use of the more reliable ΔF_n data; (iv) a systematic quantitative comparison is done between the RCI and Jarzynski ΔF estimates, showing a 6-15 fold decrease in the number of work values needed for the RCI estimates; (v) we have tested our extrapolation methods on four systems of varying molecular complexity.

For the first time, bootstrapped and sub-sampled block averaged free energies are introduced. These ΔF_n offer very smooth convergence properties allowing statistically reliable extrapolation. The ability to generate smooth ΔF_n data is critical to the extrapolation methods described here.

A quantitative comparison between the RCI extrapolated ΔF estimates and those using Jarzynski’s equality show a marked decrease in the number of work values needed to estimate ΔF when using the RCI estimates. RCI extrapolation can obtain ΔF estimates using 6-15 fold less data than the Jarzynski estimates. The linear extrapolation estimates tend to overshoot the best estimate ΔF and has a larger uncertainty than RCI extrapolation. However, the partial success of the “simple-minded” linear extrapolation does illustrate the power of the underlying idea: systematic behavior in bias can be exploited.

Other similar extrapolation methods could be developed that may offer improvement over those presented here. Such methods are currently under investigation by the authors. Future work by the authors will use extrapolation methods, such as those described here, to generate ΔF estimates for large molecular systems such as relative protein-ligand binding affinities.

IX. ACKNOWLEDGEMENTS

We gratefully acknowledge Jay Ponder for granting F. M. Y. permission to write code for TINKER to perform fast-growth free energy calculations, and to Alan Grossfield for his assistance in writing and implementing this code. We would like to thank Arun Setty for fruitful discussion and valuable suggestions. Special thanks are due to Hirsh Nanda and Thomas Woolf for permission to use the raw data for the palmitic to stearic mutation, and to David Hendrix and Chris Jarzynski for permission to use the raw data for the Lennard-Jones fluid. Funding for this research was provided by the Dept. of Environmental and Occupational Health at University of Pittsburgh, and the National Institutes of Health (T32ES007318).

[1] D. M. Zuckerman and T. B. Woolf, Chem. Phys. Lett. **351**, 445 (2002).

[2] D. M. Zuckerman and T. B. Woolf, Phys. Rev. Lett. **89**, 180602 (2002).

- [3] M. R. Shirts, E. Bair, G. Hooker, and V. S. Pande, *Phys. Rev. Lett.* **91**, 140601 (2003).
- [4] D. A. Pearlman and P. A. Kollman, *J. Chem. Phys.* **90**, 2460 (1989).
- [5] X. Kong and C. L. Brooks, *J. Chem. Phys.* **105**, 2414 (1996).
- [6] M. R. Shirts, J. W. Pitera, W. C. Swope, and V. S. Pande, *J. Chem. Phys.* **119**, 5740 (2003).
- [7] G. Hummer and A. Szabo, *Proc. Nat. Acad. Sci. (USA)* **98**, 3658 (2001).
- [8] P. A. Bash, U. C. Singh, R. Langridge, and P. A. Kollman, *Science* **236**, 564 (1987).
- [9] C. J. Woods, J. W. Essex, and M. A. King, *J. Phys. Chem. B* **107**, 13703 (2003).
- [10] J. A. McCammon, *Curr. Opin. Struct. Bio.* **2**, 96 (1991).
- [11] S. Shobana, B. Roux, and O. S. Andersen, *J. Phys. Chem. B* **104**, 5179 (2000).
- [12] B. Isralewitz, M. Gao, and K. Schulten, *Curr. Opin. Struct. Bio.* **11**, 224 (2001).
- [13] R. Bitetti-Putzer, W. Yang, and M. Karplus, *Chem. Phys. Lett.* **377**, 633 (2003).
- [14] S. Boresch, F. Tettinger, M. Leitgeb, and M. Karplus, *J. Phys. Chem. B* **107**, 9535 (2003).
- [15] J. Liphardt, S. Dumont, S. B. Smith, I. Tinoco, and C. Bustamante, *Science* **296**, 1832 (2002).
- [16] J. Gore, J. Ritort, and C. Bustamante, *Proc. Natl. Acad. Sci. (USA)* **100**, 12564 (2003).
- [17] S. Park, F. Khalili-Araghi, E. Tajkhorshid, and K. Schulten, *J. Chem. Phys.* **119**, 3559 (2003).
- [18] J. Bajorath, *Nature Rev. Drug Disc.* **1**, 882 (2002).
- [19] D. J. Abraham, ed., *Burger's Medicinal Chemistry and Drug Discovery, Sixth Ed., Volume 1* (Wiley, New York, 2003).
- [20] G. A. Lazar, S. A. Marshall, J. J. Plecs, S. L. Mayo, and J. R. Desjarlais, *Curr. Op. Struct. Bio.* **13**, 513 (2003).
- [21] W. F. DeGrado and B. O. Nilsson, *Curr. Op. Struct. Bio.* **7**, 455 (1997).
- [22] C. Jarzynski, *Phys. Rev. Lett.* **78**, 2690 (1997), *Phys. Rev. E* **56**, 5018 (1997).
- [23] J. M. Schurr and B. S. Fujimoto, *Science* **296**, 1832 (2002).
- [24] D. M. Zuckerman and T. B. Woolf, *J. Stat. Phys.*, in press.
- [25] A. Grossfield, P. Ren, and J. W. Ponder, *J. Amer. Chem. Soc.* **125**, 15671 (2003).
- [26] N. Lu and D. A. Kofke, *J. Chem. Phys.* **114**, 7303 (2001).
- [27] N. Lu and D. A. Kofke, *J. Chem. Phys.* **115**, 6866 (2001).
- [28] C. Oostenbrink and W. F. van Gunsteren, *J. Comp. Chem.* **24**, 1730 (2003).
- [29] T. Z. Mordasini and J. A. McCammon, *J. Phys. Chem. B* **104**, 360 (2000).
- [30] C. Jarzynski, *Phys. Rev. E* **65**, 046122 (2002).
- [31] R. H. Wood, *J. Phys. Chem.* **95**, 4838 (1991).
- [32] C. Jarzynski, *Phys. Rev. E* **56**, 5018 (1997).
- [33] M. A. Miller and W. P. Reinhardt, *J. Chem. Phys.* **113**, 7035 (2000).
- [34] H. Hu, R. H. Yun, and J. Hermans, *Molec. Sim.* **28**, 67 (2002).
- [35] J. C. Schön, *J. Chem. Phys.* **105**, 10072 (1996).
- [36] A. Hodel, T. Simonson, R. O. Fox, and A. T. Brünger, *J. Phys. Chem.* **97**, 3409 (1993).
- [37] D. A. Pearlman and P. A. Kollman, *J. Chem. Phys.* **91**, 7831 (1989).
- [38] A. Di Nola and A. T. Brunger, *J. Comp. Chem.* **19**, 1229 (1998).
- [39] D. A. Pearlman, *J. Comp. Chem.* **15**, 105 (1994).
- [40] O. Edholm and I. Ghosh, *Molec. Sim.* **10**, 241 (1993).
- [41] R. H. Wood, W. C. F. Mühlbauer, and P. T. Thompson, *J. Phys. Chem.* **95**, 6670 (1991).
- [42] N. Lu, D. A. Kofke, and T. B. Woolf, *J. Chem. Phys.* **115**, 6866 (2001).
- [43] N. Lu, J. K. Singh, and D. A. Kofke, *J. Chem. Phys.* **118**, 2977 (2003).
- [44] C. H. Bennett, *J. Comp. Phys.* **22**, 245 (1976).
- [45] A. Amadei, M. E. F. Apol, A. DiNola, and H. J. C. Berendsen, *J. Chem. Phys.* **104**, 1560 (1996).
- [46] G. Hummer, *J. Chem. Phys.* **114**, 7330 (2001).
- [47] J. W. Pitera and W. F. van Gunsteren, *J. Phys. Chem. B* **105**, 11264 (2001).
- [48] R. W. Zwanzig, *J. Chem. Phys.* **22**, 1420 (1954).
- [49] G. Hummer and A. Szabo, *J. Chem. Phys.* **105**, 2004 (1996).
- [50] D. A. Hendrix and C. Jarzynski, *J. Chem. Phys.* **114**, 5974 (2001).
- [51] G. E. Crooks, *Phys. Rev. E* **61**, 2361 (2000).
- [52] J. G. Kirkwood, *J. Chem. Phys.* **3**, 300 (1935).
- [53] H. Liu, A. E. Mark, and W. F. van Gunsteren, *J. Phys. Chem.* **100**, 9485 (1996).
- [54] J. M. J. Swanson, R. H. Henchman, and J. A. McCammon, *Biophys. J.* **86**, 67 (2004).
- [55] J. Hermans, *J. Phys. Chem.* **95**, 9029 (1991).
- [56] A. L. Leach, *Molecular Modelling Principles and Applications – Second Ed.* (Prentice Hall, Dorset, 2001).
- [57] T. P. Lybrand, I. Ghosh, and J. A. McCammon, *J. Am. Chem. Soc.* **107**, 7793 (1985).
- [58] D. Frenkel and B. Smit, *Understanding Molecular Simulation* (Academic Press, San Diego, 1996).
- [59] H. Nanda and T. B. Woolf, in preparation.
- [60] Thanks to Hirsh Nanda and Tom Woolf for the raw stearic to palmitic acid data, and to David Hendrix and Chris Jarzynski for the raw chemical potential data.
- [61] J. W. Ponder, St. Louis, MO (2003).
- [62] H. J. C. Berendsen, J. P. M. Postma, W. F. van Gunsteren, A. DiNola, and J. R. Haak, *J. Chem. Phys.* **81**, 3684 (1984).
- [63] H. C. Andersen, *J. Comp. Phys.* **52**, 24 (1983).
- [64] B. Efron and R. J. Tibshirani, *An Introduction to the Bootstrap* (Chapman and Hall, New York, 1993).
- [65] D. N. Politis, J. P. Romano, and M. Wolf, *Subsampling* (Springer-Verlag, New York, 1999).